REPORT DOCUMENTATION PAGE

Form Approved
OMB No. 0704-0188

1. REPORT DATE *(DD-MM-YYYY)*	**2. REPORT TYPE**	**3. DATES COVERED** *(From - To)*
Nov. 9, 2010	Final Quarterly Report STTR Phase 2	June 1, 2010 – Oct. 28, 2010

4. TITLE AND SUBTITLE

Long life, low power, multi-cell battery

5a. CONTRACT NUMBER
W911NF-08-C0064

5b. GRANT NUMBER
A2-3238

5c. PROGRAM ELEMENT NUMBER

6. AUTHOR(S)

Steve Simon – PI (mPhase)
Victor Lifton – Chief Scientist (mPhase)
ESRG – Rutgers University

5d. PROJECT NUMBER
A07-T001

5e. TASK NUMBER

5f. WORK UNIT NUMBER

7. PERFORMING ORGANIZATION NAME(S) AND ADDRESS(ES)

mPhase Technologies
150 Clove Rd
Little Falls, New Jersey
07724

8. PERFORMING ORGANIZATION REPORT
4ALV9

9. SPONSORING / MONITORING AGENCY NAME(S) AND ADDRESS(ES)

US Army Research Office
P.O. Box 12211
Research Triangle Park, NC

10. SPONSOR/MONITOR'S ACRONYM(S) NUMBER(S)
DCMA Munitions and Building 1, ARDEC
Picatinny, NJ 07806-5000

12. DISTRIBUTION / AVAILABILITY STATEMENT
Approved for public release; distribution unlimited.

13. SUPPLEMENTARY NOTES
The views, opinions and/or findings contained in this report are those of the author(s) and should not be construed as an official Department of the Army position, policy or decision, unless so designated by other documentation.

14. ABSTRACT
Report developed under STTR contract W911NF-08-C-0064.

This award was based on the successful results of a Phase 1 STTR award to continue with the development of a small footprint, reserve style lithium based arrayed battery containing more than one cell that can be individually addressed, and that can provide long storage life and long term power for continuous use in powering micro electronic devices.

The enclosed 6th quarterly report is the final summary report and encompasses the work perform by the team from June 2010 through Oct 28.2010 as a well as the

15. SUBJECT TERMS

16. SECURITY CLASSIFICATION OF:	**17. LIMITATION OF ABSTRACT**	**18. NUMBER OF PAGES**	**19a. NAME OF RESPONSIBLE PERSON**
			Steve Simon

a. REPORT	b. ABSTRACT	c. THIS PAGE			19b. TELEPHONE NUMBER *(include area code)*
UNCLASSIFIED	**UNCLASSIFIED**	**UNCLASSIFIED**1	UL	12	973-638-2451

Oct 28, 2010

Contract: W911NF-08-C0064
CLIN Invoice: #0001 and #0002
Purchase Request Number: 54927CHST208222
PROJECT: A07-T001
Proposal # A2-3238

Project Title: Long life, low power, multi-cell battery.

Eight Quarterly Report (Final Report): **- June 1, 2010 through Oct, 28, 2010 -**

Objective

This award was based on the successful results of a Phase 1 STTR award to continue with the development of a small footprint, reserve style lithium based arrayed battery containing more than one cell that can be individually addressed, and that can provide long storage life and long term power for continuous use in powering micro electronic devices.

The enclosed report encompasses the work performed by the team from through June 1 through Oct 28, 2010, and is the final and concluding report of the project.

Accomplishments for Reporting Period

Work tasks undertaken this period – June 1, 2010 – Oct 28, 2010

Task #	Task	Start	Target Milestone	Status
1	Develop deposition parameters and testing procedure of hydrophobic coating on porous membrane and testing of electro wetting transition in final battery assembly.	May 2009	Completed Oct. 28, 2010	Successful electro wetting observed in final samples provided by Silex foundry. Longer term stability testing has been ended with completion of project.
2	**A.** Major task will be the design and development of the complementary glass structures that provide for the containment walls that hold the electrolyte.	Sept 2009	Task **A** Completion August 2010	**A.** Glass wafers successfully ultrasonic machined and patterned with gold. Results of processing indicated that further yield rate improvements are achievable with additional control during machining.
	B. Major task will involve the use of an anodic bonding approach to fuse the silicon substrate containing the micro channels to the glass grid wall structures described above.		Task **B**. completed, anodic bonding approach used on top glass and silicon layers	**B.** Final wafers of silicon and glass grids successfully bonded using anodic processing approach. Some wafers were lost during dicing step due to incorrect alignment of materials in wafer level bonding tool.
	C. Testing of PerMX polymer bonding material as an alternate approach to using thermocompession bonding. PerMX was		Task **C**, Complete Sept. 2010. PerMX	**C.** Bonding tests and alternate approaches using polymer laminate, (PerMX) to bond

	considered as an alternate approach if temperatures required during thermal bonding was to high (above 170 C) and effected lithium and floropolymer hydrophobic coatings. PerMX testing procedures involves tensile strength bonding.		approach tested but was not used in final assembly.	silicon to glass was conducted on test material with partial success in finding correct parameters to get PerMX laminate to adhere to silicon at foundry. Material appears to be favorable, but additional testing is required, outside the scope of the Phase II award. Test results of shear strength testing on PerMX samples conducted over a six month period indicted that the bond strength of PerMX was reduced when exposed directly to electrolyte.
3	Development of bottom layer comprised of processed silicon and glass substrates that contains electrode stack.	April 2010	May 2010 – Short loop test completed.	**A.** Titanium metalization short loop testing of the top surface of silicon substrate to protect silicon from lithiation. Short loop test input used to determine pin hole free deposition of Ti metal for final assembly
4.	Vapor pressure testing to determine if electrolyte vapors impact lithium via through hole pores in silicon membrane.	April 2010	Task **A**. First round of testing completed, results kicked off pre-passi vation testing completed.	**A.** Tests determined that long term vapor exposure to lithium by PC electrolyte could impact the performance of the cell.

			Oct. 2010 Task **B**. Pre-passivation testing using inorganic and organic approach completed Oct. 2010	**B.** Testing determined if pre-passivation of lithium mental could help improve performance of the cell due to vapor exposure by electrolyte. Test results indicated that prepassivation using both inorganic and organic approach does help, but the effects are relatively small. During testing, it was determined that using nitrogen to prepassivate lithium was more difficult to control than using the dip coated method of lithium immersed in vinylene carbonate. Test results indicated that incremental improvements were not of high value and lithium electrodes used during final assembly were not pre passivated.
5,	Task **A**, Assembly of final batteries, bonding of top and bottom sub assemblies.	Oct, 2010	Task **A** Completed Oct. 2010	Successfully bonded top and bottom assembly using Surlyn polymer material from Dupont. Mixed results getting acceptable

				thermo compression bonding to work when filled with electrode stack. Tests results indicate that higher bonding temperatures will be required , with would involve the need for using lithium alloy material rather than pure lithium as anode.
	Task **B**, Insertion of electrode stack	Oct. 2010	Task **B** Completed Oct. 2010	Successfully built electrode stack and inserted inside electrode cavity.
	Task **C**, Addition of electrolyte and sealing fill holes.	Oct. 2010	Task **C** Completed Oct. 2010	Successfully added electrolyte to battery reservoir. Results of battery assembly indicate that filling reservoir completely full will require some redesign to top cap assembly and fill hole area to help improve tendency of air bubbles from forming inside battery reservoir during filling step.
	Task **D**, Attachment of printed circuit boards.	Oct. 2010	Task **D** Completed Oct. 2010	Successfully attached top and bottom printed circuit boards to battery samples.
6	Discharging cells.	Oct. 2010	Task Completed	Discharge characterization

			Oct. 2010	started. Preliminary results indicate that the cells are capable of supporting discharge currents in excess of those required by the original solicitation. Further testing is required to assess 30-year lifetime.

TASK 1 Hydrophobic coatings.

During this timeframe, the work was completed on testing the stability of the hydrophobic coatings as described in the previous reports. For reference, we have several types of coatings under test:

- Teflon based, with various concentrations of Teflon, 1 and 3% by wt.
- Vapor deposited coatings from Integrated Surface Technologies, based on self-assembled monolayer, reinforced with nanoparticles (IST) – already failed and excluded from further testing.
- Dip coatings of various polymers from Cytonix Corp., specifically optimized for the chemical stability in organic solvents.
- Dip coating samples from Cytonix prepared to exhibit superhydrophobic behavior due to presence of nanoparticles in the solution (MP1604PS).

So far, we have accumulated up to **315 days** of continuous exposure to the electrolyte at 60 ^{o}C (interrupted only to wash and measure the samples on the contact angle tool. These times are not included in the overall time of exposure). As can be seen from Figure 1, coating of Teflon on SiO_2 substrate still survives after more than 310 days of continuous exposure. The data points seem to fluctuate around a contact angle value of ~ 120-130 degrees, which gives us confidence in the long-term prospect of such coating, especially at lower temperature of 20-30 ^{o}C. A new batch of Cytonix coatings so far shows good stability after about 160 days of exposure and the data are given in Figure 2. It is acknowledged that the exposure period for the Cytonix coatings are too short to draw long term predictions and we will continue monitoring these samples. Note that the Cytonix coating containing nanoparticles shows higher contact angle ~ 130 deg vs coatings free of nanoparticles ~ 120 deg. This contact angle observation is expected as the nanoparticles help achieve nearly superhydrophobic state as evidenced by the large value of the contact angle. Such state is remarkable in its very low liquid-solid area of contact, which leads to a smaller fraction of the solid surface and the coating itself exposed to the electrolyte. As a result, we can expect lower failure rate in such system.

Given good stability of the Teflon coatings in the electrolyte at 60 ^{o}C, we can expect that it would translate into an even longer stability in the electrolyte at room and lower temperatures.

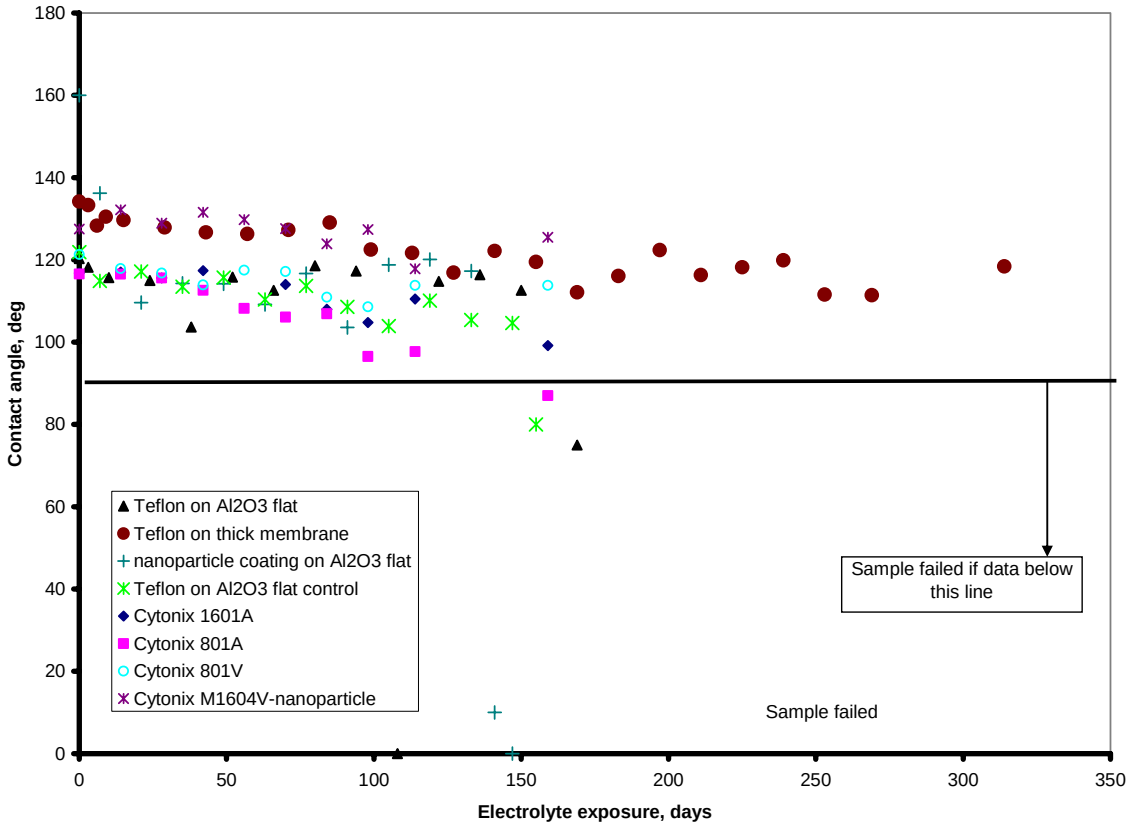

Figure 1. Contact angle on various coatings on flat and membrane samples.

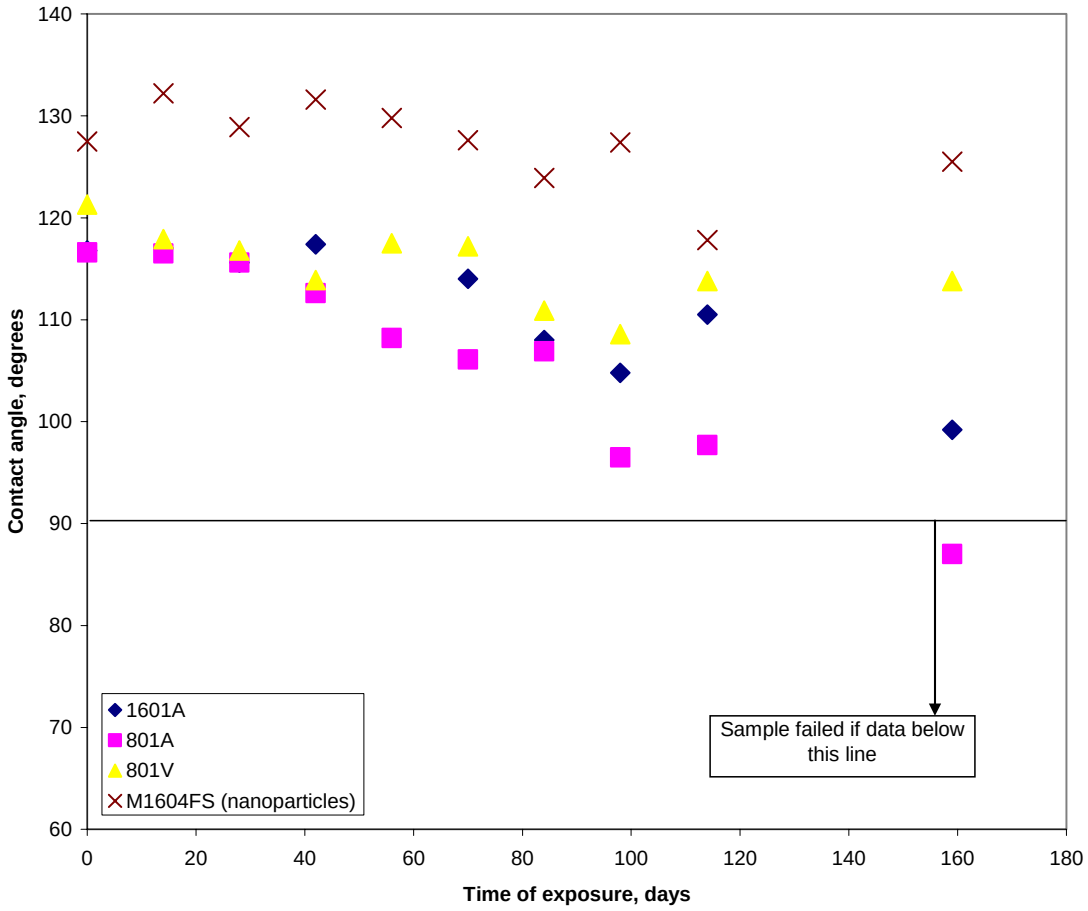

Figure 2. Contact angle as function of time on the second batch Cytonix coatings.

Conclusion*: As a result of Phase II funding, design and fabrication principles have been established and proven by fabricating membranes at an external contract foundry. Superhydrophobic membranes are now routinely fabricated by the team and are capable of supporting a wide range of aqueous and organic solvents used in Li and non-Li battery technology. We have access to a supplier of the membrane that can fulfill our requests on a short notice with high quality and high yield. Hydrophobic coatings based on Teflon AF material show the best stability in the electrolyte for over 310 days of continuous exposure at 60 ^{o}C. They are chosen as the coatings of choice for this project.*

Task 2A Bonding tests.

During this period we completed short loop testing the various bonding approaches on sacrificial samples prior to the final design. Initial testing involved anodic

bonding and alignment of the top glass reservoir layer to a silicon substrate, which in the final design was substituted by using the porous silicon honeycomb membrane structure. In general, the anodic bonds appear to be stable on our test wafers and the anodic process was used in the final assembly.

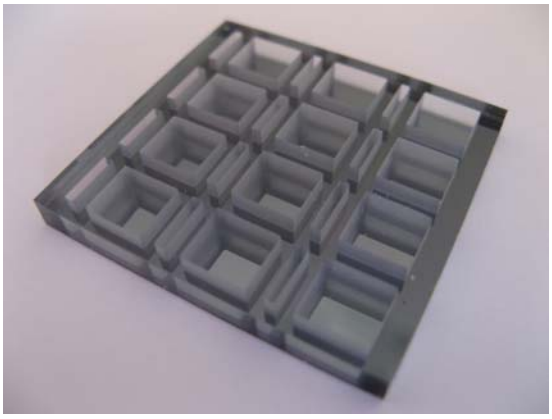

Figure 3. The figure depicts an anodic bond of the glass grid reservoirs to a silicon substrate which acts as a stand-in substrate for the silicon porous membrane.

Task 2B Adhesive bonding strength evaluation

As was reported in the previous reports, the main bonding method chosen for this project was initially a thermocompression bond. The method is well known in the MEMS community and consists of bonding substrates using Au bond layers at moderate pressure and temperatures in 200-400 ^{o}C range. This method typically forms hermetic, reliable bonds between parts and was therefore chosen for this project. One potential issue in implementing this technique in our work is the need for relatively high bonding temperature (e.g. 400 ^{o}C that exceed the melting temperature of Li anode, 181 ^{o}C).

As an alternative to thermocompression bonding, we identified adhesive bonding using a specially developed material by DuPont called PerMX. The adhesive bonding method using this material does not require high temperature and can be performed at 100-150 ^{o}C. The material itself can easily be applied to various substrates (patterned and nanostructured) and shows excellent adhesion to Si, silicon oxide, nitride and metals. It appears to be an interesting choice for implementation, as it may simplify the processing and offer wide processing conditions for materials that would be adversely affected by higher temperature bonding ranges.

One unknown aspect of PerMX properties prevents it from an immediate integration in our process flow – its chemical stability in contact with the electrolyte. We have already reported that most of the polymers and plastics tend to be adversely affected by the electrolyte by dissolution, swelling, loss of adhesion to the substrate. To address this issue, we created a set of specially designed samples to investigate PerMX stability in the electrolyte.

The samples consisted of silicon and glass substrates bonded together using a layer of PerMX photolithographically patterned with the same pattern as used in the design of the 3x4 battery array. This was done to make sure all of the bond geometric parameters such as width, length and overall area would be same as in the battery samples. This allows direct comparison with the target structures. The samples were diced into 31x33 mm rectangles resembling battery samples and subjected to the electrolyte soak at 60 ^{o}C. Several samples were set aside as baseline (un-exposed to the electrolyte) to measure the bond strength If any PerMX degradation occurs due to its chemical reactions with the electrolyte, it would manifest itself by a reduced bond strength as compared to the bond strength in the baseline non exposed bonded state.

To measure bonded strength we used shear test method, where a sample was glued to two metal plates and pulled apart in an Instron-type tool. Such shear strength testing is widely used in the MEMS community and has been shown to give reliable information on the bond strength. A schematic representation of the test is given in Figure 4.

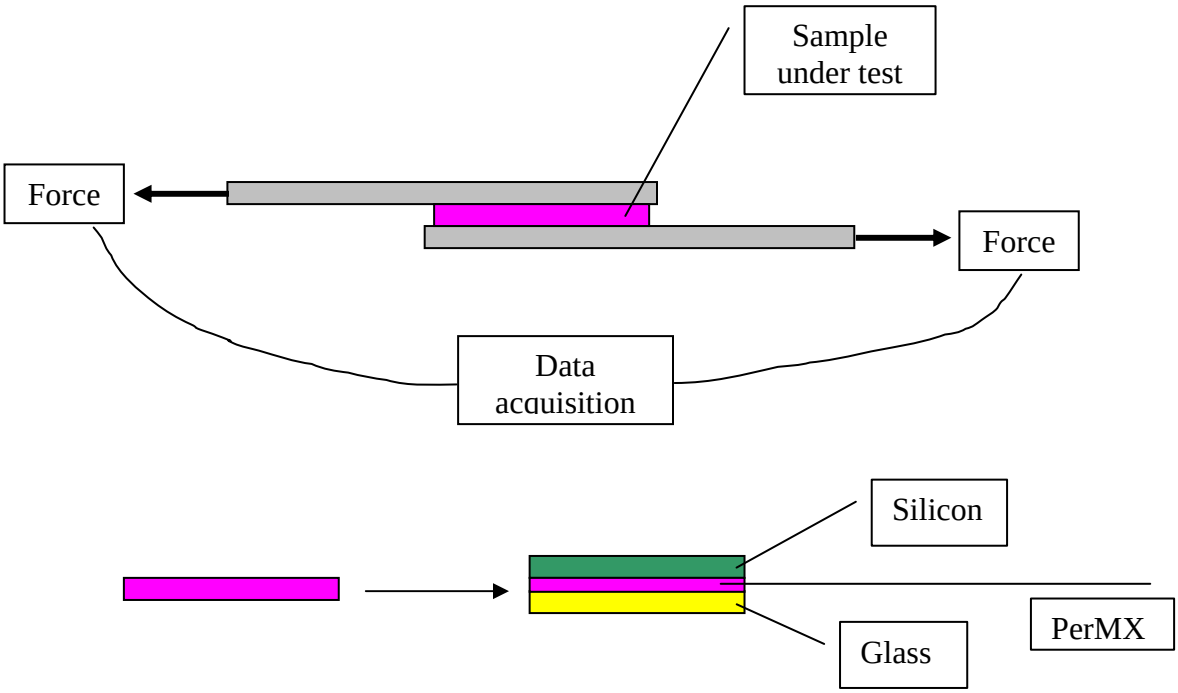

Figure 4. Schematic representation of a system for measuring shear strength of the bond. A sample under test consists of silicon and glass plates glued together by PerMX.

In such configuration the sample under test must be attached to the plates using some form of clamping and mounting procedure and is typically accomplished by using an adhesive such as instant glue. However, since the bond strength of this joint is unknown, it is impossible to predict if such adhesive glue will provide bond strength sufficient to withstand the shear test. In case the bond under test is stronger than the attachment bond, the latter will fail first and prevent accurate collection of data for the bond strength. The sample can fail at the adhesive interface of interest or at the interface where the sample is attached to the mounting plates. We want to avoid failure at the mounting plates.

Therefore, as the first step in our study, we characterized the bond of several types of glues and epoxies to ascertain their strength. The samples for this work were pieces of borosilicate glass, identical to those used in silicon-to-glass samples for our battery fixture design, cut to the same size of the 3x4 battery array. To qualify the adhesive, the glass sample was glued to the plate using individual glue sample, left to dry and pulled apart using the tensile strength tool.

The results are summarized in the Table 1 below. Only one glue sample tested (Loctite 406) was determined unsuitable for further use, it has failed at the glue interface where the glass sample was attached to the plates. In contrast, in all other samples, it was the glass sample that cracked and fractured during the shear tests – glue interfaces were stronger then the glass itself. As a result of this preliminary screening we elected to use Scotch Weld DP 810, a two-part acrylic adhesive for mounting samples under test to the metal plates. See Figure 5 for the photos of the samples after the shear test.

Adhesive	Shear strength, MPA
Loctite 406	0.5
	0.7
Loctite 415	4.3
	4.9
Loctite 493	3.4
	3.5
Scotch Weld DP 125	3.9
	4.6
Scotch Weld DP 810	10.9
	11.4
Loctite E-00CL	3.4
	3.6
Loctite E-20HP-2	9.1
	11.3

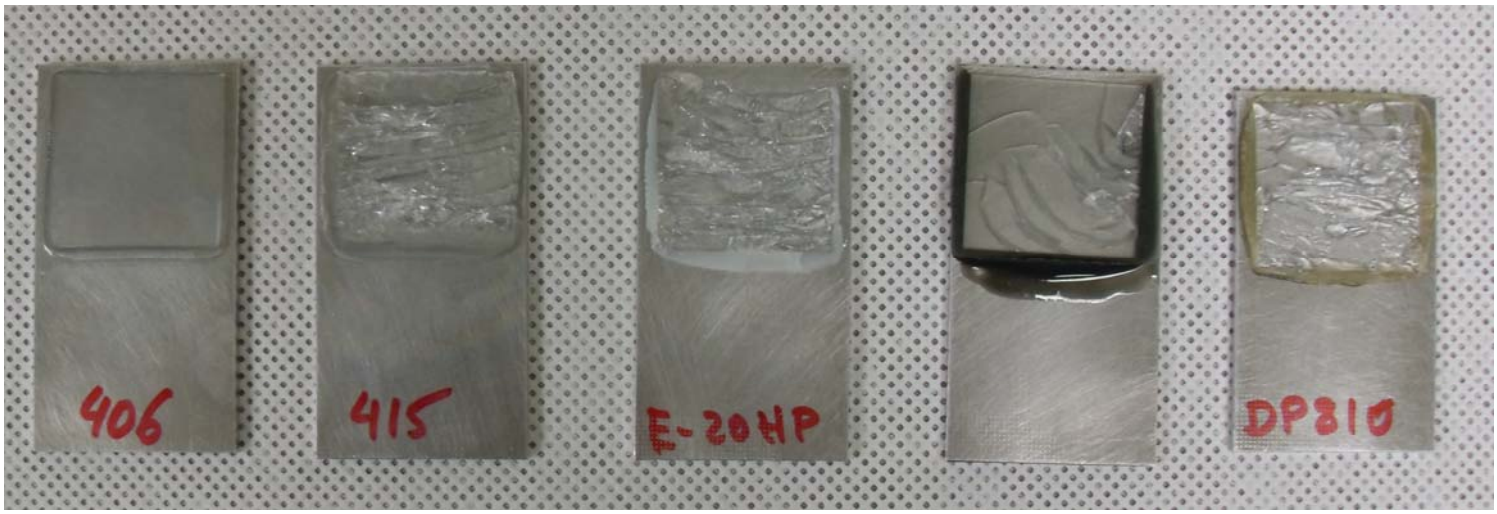

Figure 5. Shear strength test samples of various adhesives after the test. Notice that Loctite 406 sample (on the left) shows no damage to the glass sample; in this particular case the glue does not have sufficient shear strength to withstand the loads used. The rest of the samples show significant damage in the form of fracture in the glass samples. In this instance, all adhesives have adequate shear strength to be used as the mounting adhesives for the actual test samples.

Once we identified the glue to withstand shear stresses applied during a typical shear strength test, we proceeded by testing PerMX samples that were not exposed to the electrolyte (as-bonded state). The data are presented in Table 2 below and labeled as "Dry PerMX patterned or Dry PerMX unpatterned". The only difference between the two sets of samples is that in the former case, the sample has been patterned into a 3x4 pattern, whereas the latter case, the sample was a flat piece of PerMX, bonding glass to silicon. This reference is the baseline bond strength (~ 17 MPa) that can be expected from the PerMX bond that was not degraded by any unwanted reactions with the electrolyte. For comparison, other adhesives tested at earlier stages of the project typically failed (most often completely dissolved) after only 3 days of exposure to the electrolyte.

The results of the shear tests are also presented in Table 2 labeled as "PerMX. As seen, the bond strength is ~ 15 MPa, very close to the initial value of the bond strength, within the experimental error of the test. Additional samples were exposed to the electrolyte and tested after accumulating at least 30 and 60 days at 60 ^{o}C. Results of the tests indicate that the PerMX coatings have greatly reduced bond strength after 60 days of exposure when in direct contact with the electrolyte.

	Force, N	Area, mm^2	Shear strength, MPa
PerMX after 180 days	582	464.88	1.25
PerMX after 180 days	458.5	464.88	0.99
PerMX after 101 days	3265	464.88	7.02
PerMX after 101 days	3446	464.88	7.41
PerMX after 64 days	3214	464.88	6.91
PerMX after 19 days in LiClO4 -1	8225.79	464.88	17.69
PerMX after 19 days in LiClO4 -2	6007.07	464.88	12.92
Dry PerMX unpatterned -1 #3	10186.23	634.75	16.05
Dry PerMX unpatterned -2 #6	9477.40	681.88	13.90
Dry PerMX patterned - 1	8670.14	464.88	18.65
Dry PerMX patterned - 2	9868.71	464.88	21.23

As can be seen from Figure 6 taken after the sample was tested for shear strength, PerMX adhesive tends to peel off the glass substrate and remain on the silicon substrate. Therefore, if the improved adhesion will be required, it would suggest that PerMX adhesion to glass needs to be improved. In fact, it may be improved by depositing a metal underlayer, as it is suggested by the manufacturer that PerMX's adhesion to metal may be stronger than to other materials. In addition, fracture bands can be seen on the glass substrate (as wavy lines going across the sample). It indicates that prior to the failure at the PerMX-glass interface, glass experienced stresses that nearly exceeded its fracture toughness. This fact shows that the strength of the PerMX-glass and PerMX-silicon bonds is very close to the fracture limit of the glass substrate itself – an excellent manifestation of the strength of the PerMX bond.

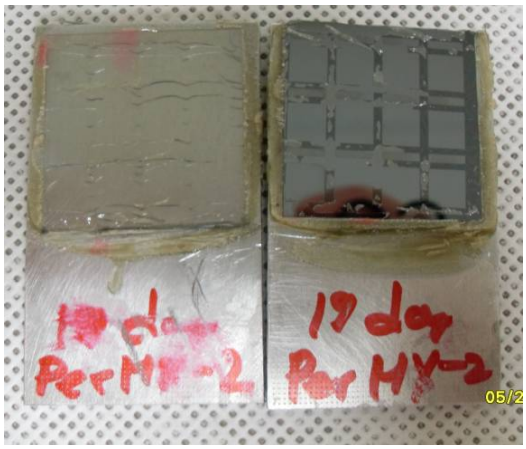

Figure 6. A sample of PerMX exposed to the electrolyte for 19 days at 60 ^{o}C after the shear strength test.

As seen from the above table, the bond strength after 6 months of exposure is reduced to about 1 MPa. While it may still be enough to keep the samples from falling apart, such reduction is troubling, as it may eventually lead to an internal leak of the electrolyte inside of the packaged battery and therefore this assembly method should not be used in this particular project. However, we want to emphasize that in other MEMS projects not requiring the use of aggressive chemicals as is often the case, such assembly method may become invaluable, as it provides for clean-room compatible assembly processing using standard equipment (lamination and photolithography).

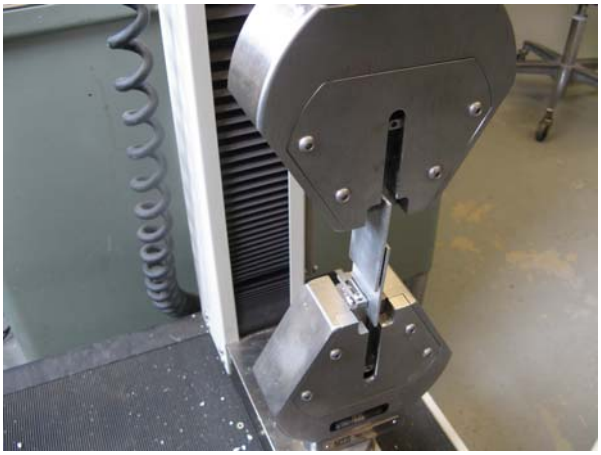

Figure 7. Experimental set-up using tensile strength measurement tool.

Conclusion: *During phase II, we have successfully accumulated an extensive body of experimental results involving various bonding materials, which has yielded successful approaches for developing processing steps for the assembly of the multi-stack designs constructed out of layers of silicon and glass. We have tested approaches using anodic bonding, thermo compression bonding and polymer bounding, using both PerMX and Surlyn low melt materials.*

TASK 3 – Development of bottom cap electrode containment structure

A short loop test was conducted to determine the method to protect the inside surface of the silicon substrate that comprises the bottom portion of the fixture that holds the CFx and Li electrodes. Because lithium has a propensity to diffuse into the silicon substrate over time, and form Si-Li alloys, resulting in an expansion and cracking of the silicon substrate, a pin hole free interface protection layer is required on the silicon substrate. Chosen for compatibility with lithium and the electrolytes, Ti metal was deposited on the inside surface of the silicon layer, at a thickness of 1 micron, to create a pin hole free interface. FESEM imaging was used to confirm the topology of the Ti deposition and electro-chemical testing was used to validate that there we no pin holes in the Ti layer where lithiation could occur with the Si substrate. The results of this short loop test were

used to determine the Ti deposition thickness used for the final assembly structure. Figure 8, show the results of the test procedures.

Close examination of the Ti film structure using FESEM showed the presence of small, nano-sized pores in the Ti coatings. The examination revealed a relatively uniform deposition of Ti of approximately 100nm, primary grain size on the Si surface, typical of a grain structure of a sputter deposited film (Figures 8-9). The Ti film was relatively uniform with only a very small number of defects. Energy Dispersive Spectroscopy, (EDS) realized the presence of Ti and Si. This was not an indication of pores within the Ti, but rather the analysis depth of the probe that is usually 1000nm or so, well beyond the thickness of the Ti cover layer so that it reaches the Si substrate as well. Within the secondary beam some bright spots were identified, but EDS mapping proved that this was not due to a composition change of the T-Si ratio. If the pores do not form an interpenetrating network, their presence will not be detrimental and the Ti coating will protect Si from lithiation.

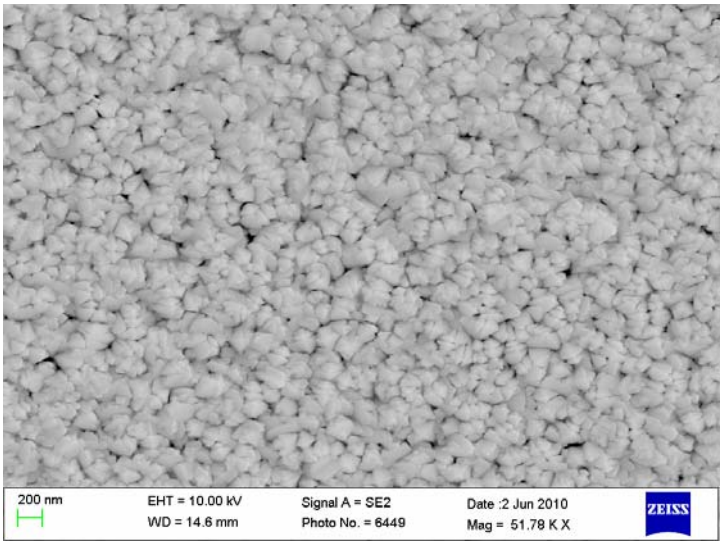

Figure 8. SEM overview of the Ti sputter film.

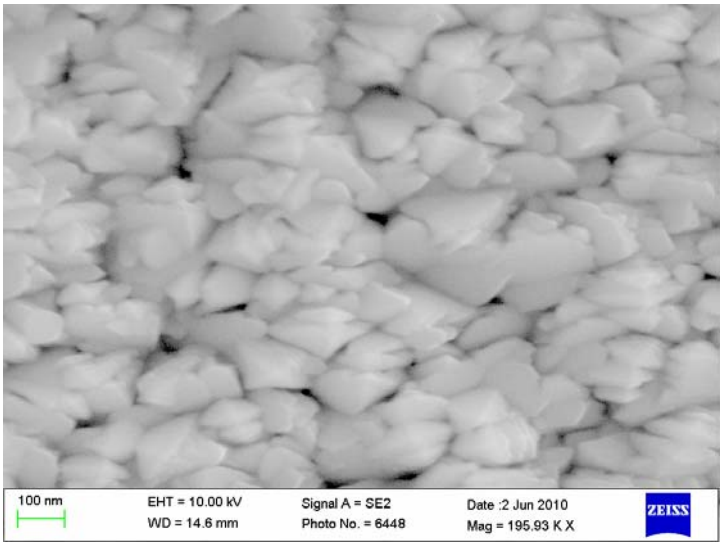

Figure 9. Details of the grain structure of the Ti film. Notice dark spots on the image representative of the pores in the film. The pores are roughly 10-50 nm in diameter. It is not known if they form an interconnected network extending all the way down to the Si substrate.

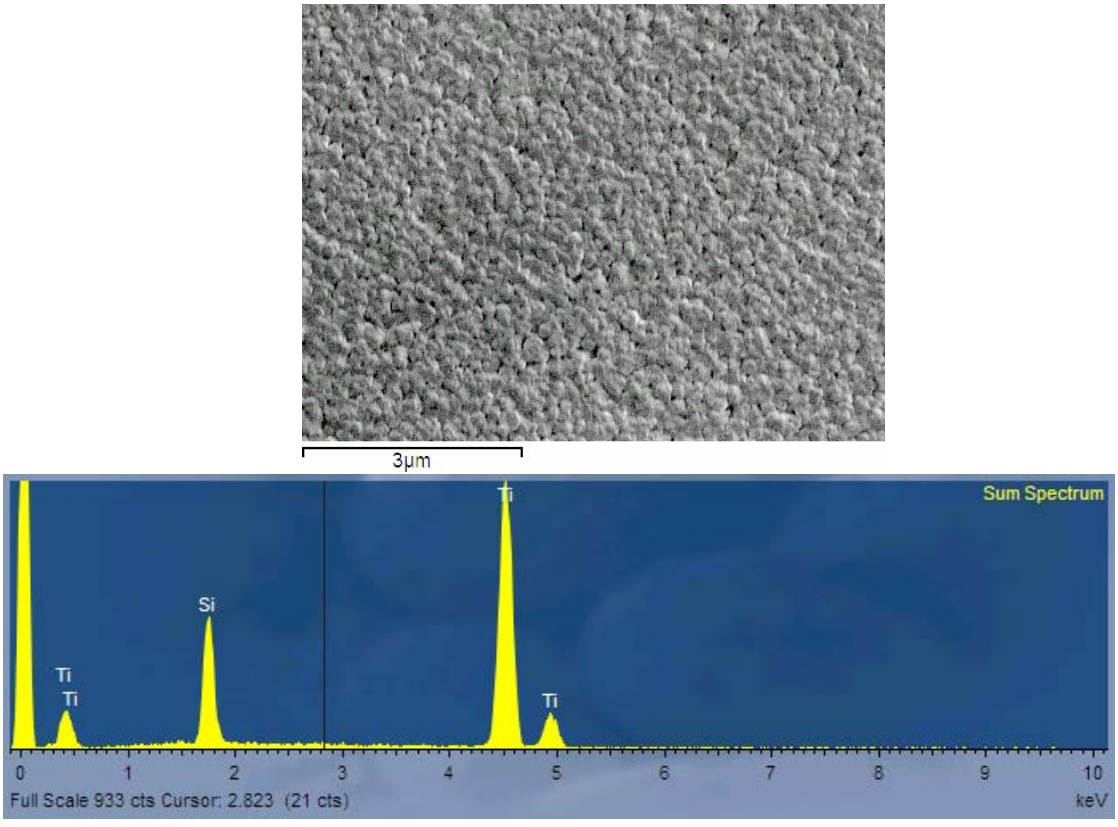

Figure 10. Both Ti and Si peaks are present in the EDS scan across the Ti film. The presence of Si may be explained by the excitation of the Si atoms in the substrate and the corresponding X-rays reaching the detector through the 1 um thick Ti film.

We followed up the FESEM analysis by using a more definitive cyclic voltammetry test to determine if lithiation was occurring through the Ti layer. A Ti coated sample of Si was placed into an electrolyte of LiClO4 EC:DMC vs Li metal. The cell was designed to limit the contact of the electrolyte with the uncoated edges of the Si substrate. The cell was discharged at a very slow current of 0.1 mA. If Si alloys were to form, this would occur at approximately 0.3V. As can be seen the Figure 11, a plateau occurs below 0V which is associated with Li metal plating on top of the Ti, as would be expected, and no plateau associated with electrolyte contact with the Si was evident.

The data suggests that the Ti coating is pore free and should be an acceptable barrier against the electrochemical reaction of Li with Si to form destructive LixSi alloys.

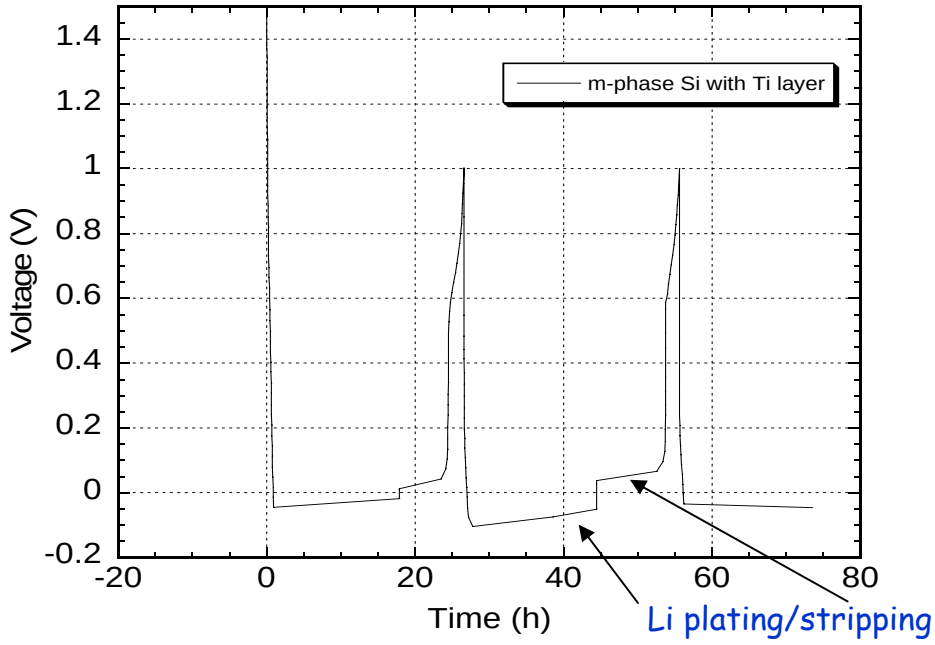

Figure 11. Cyclic voltammetry test indicate that no lithiation occurred. If Si alloys were to form, a plateau at 0.3 V would occur.

Based on the combination of results of both FESEM and electrochemical tests, we decided to take the prudent approach and implemented the procedure to potentially avoid forming a continuous network of pores, by performing an interrupted deposition of the Ti film. Our target deposition was 1000 nm thick Ti film, and it was deposited using the approach of laying down 200 nm of Ti, stopping the process and restarting the process to grow another 200 nm until the full 1000 nm thickness was reached, (5 times x 200 nm in each run). This enabled the deposition tool to coat the sample more uniformly and prevented large interconnected pores from forming.

Conclusion: *During Phase II, we successfully developed an approach to avoid lithiation of the silicon electrode substrate, by protecting and isolating it with 1 um thick Ti layer. Results of testing indicate that controlled multi-layered deposition, with pauses between each metallization layer yields the best protective results.*

TASK 4: Electrolyte vapors permeation through the porous membrane and their effects on Li anode.

A major advantage of the reserve battery is the potential to provide for a very long shelf life prior to battery activation. Because the silicon membrane is intentionally designed to be porous, allowing the electrolyte to flow once triggered, we conducted an investigation to determine if the vapors of the electrolyte could potentially interact with the lithium electrodes prior to activation, thus reducing the expected performance of the electrodes once the battery was triggered. The tests were conducted by exposing lithium metal electrodes to the vapors of various electrolytes, $LiClO_4$, PC and DMC, in a sealed Swagelok container for one, two a four week periods, Figure 12. The vapor exposed lithium electrodes were first visually observed to determine if passivation had occurred to the surface layer of the lithium and then tested using a Maccor test analyzer, by charging and discharging the electrodes to determine capacity baselines and deviations from the baseline samples, Figures 13-15.

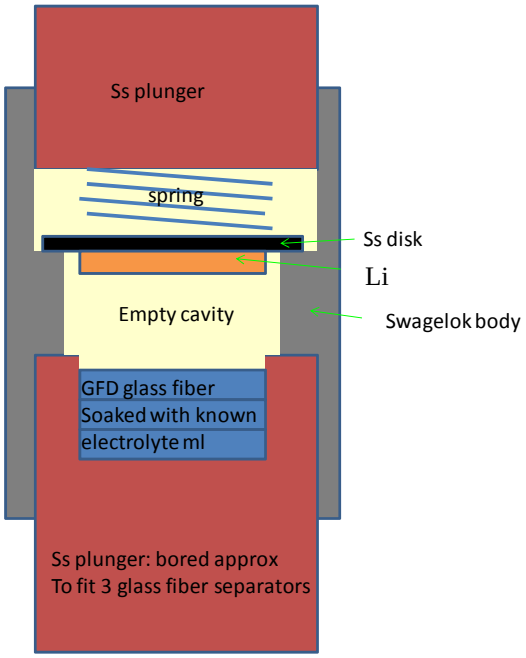

Figure 12. Test fixture to determine the effects of vapor pressure on lithium. Test fixture is used to simulate potential lithium exposure to the electrolyte through the honeycomb porous membrane.

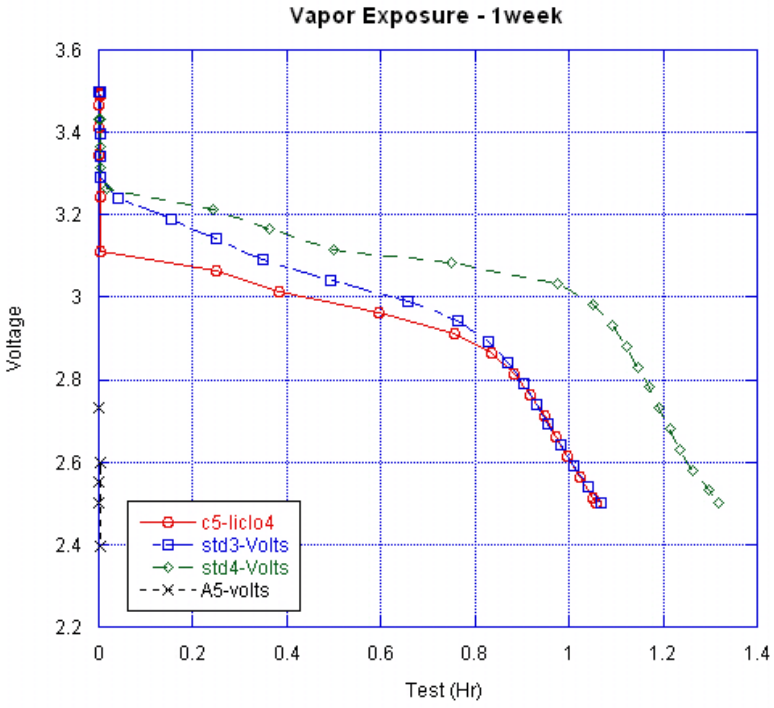

Figure 13. Vapor exposure Test, $LiClO_4$, PC and DMC , 1 week.

Capacity:

- red ($LiClO_4$) = 105.6mAh/g
- blue (std) = 106.6mAh/g
- green (std) = 131.5mAh/g

During the tests the following observations were made:

- Initial voltages around 3.45V.
- Lithium exposed to PC (black symbols), had an initial voltage of 2.7V with immediate discharge with any current added. Lithium disc very gray and corroded. 1 of 2 broke into pieces during assembly.
- Initial IR drops suggest impedance.

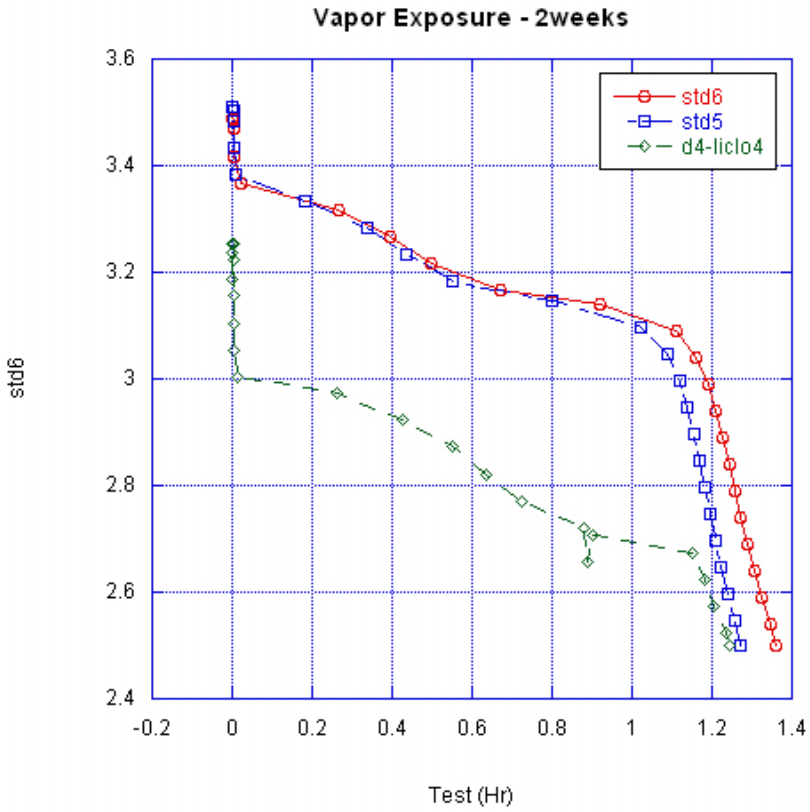

Figure 14. Vapor exposure Test, $LiClO_4$, PC and DMC, week 2.

Capacity:

- red (std) = 127 mAh/g
- blue (std) = 136 mAh/g
- green ($LiClO_4$) = 124 mAh/g

During the second week of testing the following observations were made:

Comments:

- Initial voltages of standards at 3.5V; D4 w/ $LiClO_4$ exposure was 3.3V
- Cells exposed to DMC for 2 weeks had slight but uniform grayish discoloration. Initial voltage of 1.4V and unable to discharge. Cells exposed to $LiClO_4$ had faint streaks of grayish discoloration, but overall remained shiny Lithium.
- Initial IR drops suggest impedance issue.

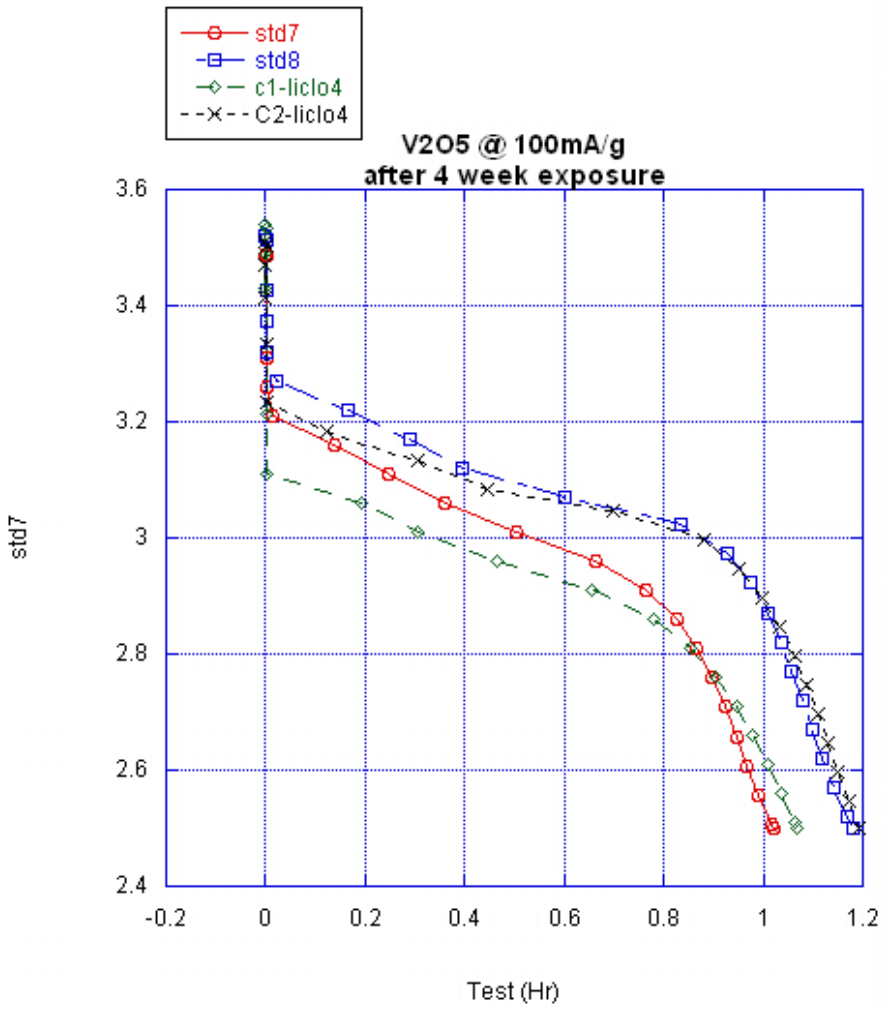

Figure 15. Vapor exposure Test, LiClO4, PC and DMC, week 4.

Capacity:

- red (std) = 102 mAh/g
- blue (std) = 117.6 mAh/g
- green ($LiClO_4$) = 106.5 mAh/g
- black ($LiClO_4$) = 119 mAh/g

Observations at the end of 4 weeks were as follows:

- Initial voltages of all cells at 3.5V
- Similar uniform gray corrosion on PC cells. Initial voltage of 0.6V and could not discharge.
- Cells exposed to $LiClO_4$ had more streaks of grayish discoloration, but still had exposed shiny Lithium.
- Initial IR drops suggest impedance issue.

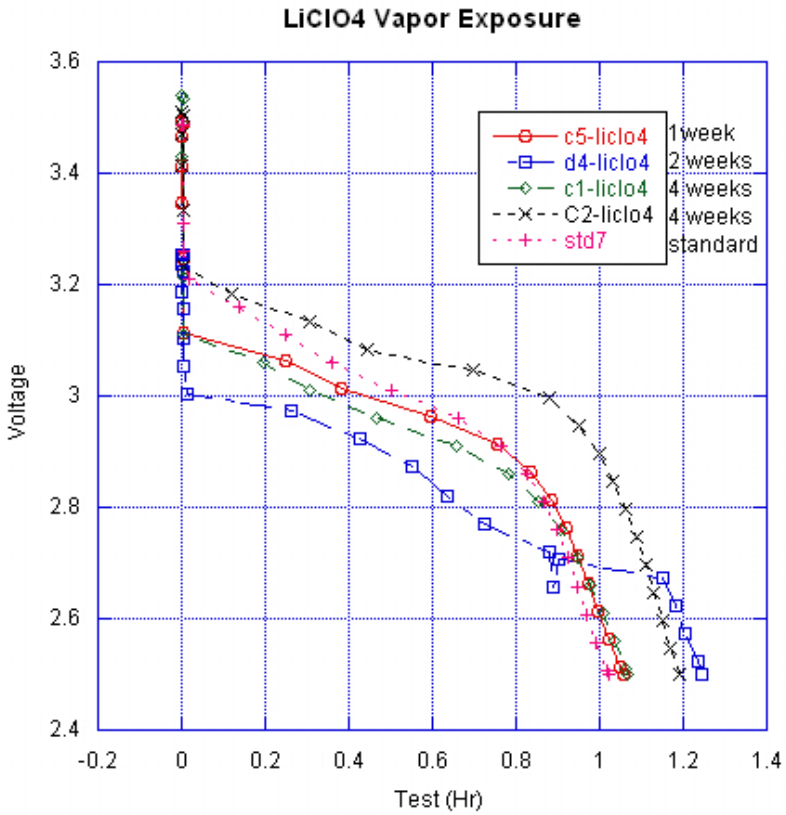

Figure 16. Samples exposed to $LiClO_4$

These results indicate that the electrolyte vapors will chemically react with the metallic lithium and cause unwanted degradation in the performance of the battery unless protective pre-passivation of the lithium electrode is carried out. Among the electrolytes tested, pure solvents such as PC tend to degrade the electrode the most. $LiClO_4$-based electrolyte (with EC-DMC as the solvent) tends to slow down the degradation and gives guidance on how to address this issue. We speculate that the mechanism by which the degradation is slowed down in this case is due to the formation of an SEI layer on the surface of lithium.

Task 4.1 Pre-passivation lithium electrode approach.

The exposure of the lithium surface to the electrolyte vapors, induced by the linear and cyclic carbonate solvents as described above, indicates on the gradual formation of a resistive decomposition layer on the surface of the lithium metal. Unfortunately, the solvents originating the most vapors are those which are known not to form solid, self limiting solid electrolyte interphases. To combat this challenge, the team has taken an approach during the final reporting period to prepassivate the surface of the lithium with a layer which would be impermeable to solvent vapor attack. We investigated two approaches, the first is based on the formation of an organic interphase, and the other is focused on an inorganic approach.

The organic approach focuses on the prepassivation of the lithium surface with vinylene carbonate. Vinylene carbonate is known to aggressively form tight, polymerized passivation layers. Such materials have shown great promise as additive materials in lithium ion batteries to passivate negative electrode materials from aggressive attack by thermodynamically unstable solvents. In our case, the lithium is pretreated in a solution of vinylene carbonate to form an electrochemically polymerized passivation layer before the lithium is inserted into the cell.

The inorganic approach is focused on the development of an inorganic solid state lithium ion conductor on the surface of the lithium metal. This layer is impermeable to the electrolyte solvent and prevents the contact of the solvent vapor with the lithium. As these layers are excellent electronic insulators, no electron transfer can be made to reduce the vapor. Therefore, the vapor will not electrochemically react on the surface of the inorganic passivation layer. The first approach investigated was the formation of highly ionically conductive Li_3N layer.

Although the initial results to grow a uniform formation of Li_3N layer on Li looked promising, (Figure 17), a more careful analysis indicted that is was difficult to control the uniform distribution of the growth and more resources would need to be allocated to better control the uniformity of the experiment.

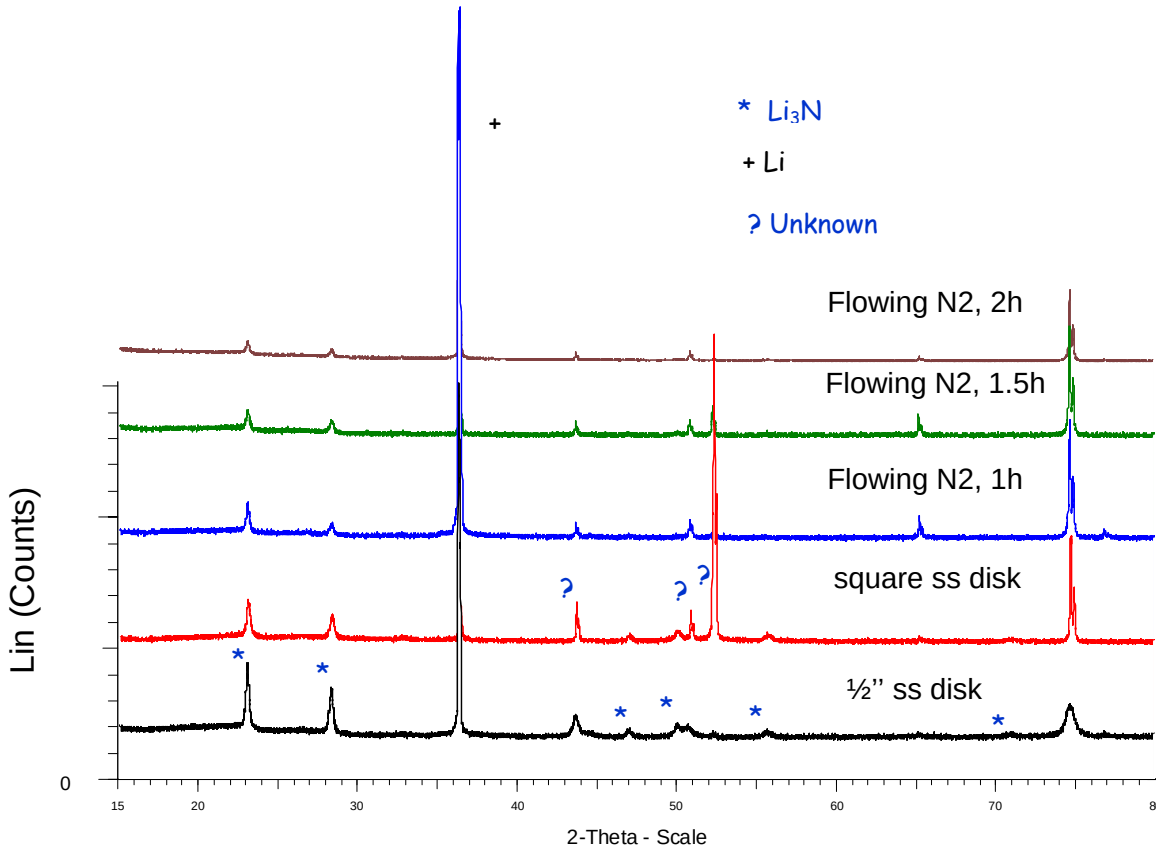

Figure 17. Chart depicts the attempt to form a uniform pre passivation distribution of Li_3N on the Li sample. Tests results indicated that they were not uniform enough to evaluate their effectiveness.

The second approach was the use of vinylene carbonate (VC). VC forms an instantaneous SEI layer on the surface of the Li which would then possibly limit the effect of the solvent vapor exposure in the reserve cell. Lithium was pre-reacted with VC for various times before its introduction into the electrolyte vapor test cell at various temperatures including 70 ^{o}C. FTIR peaks at approx 1800 and 1100 cm^{-1} indicate the presence of organic bonds related to VC polymerization on Li, Figure 18. In many cases the use of VC resulted in a slightly improved electrochemical activity of the subsequently fabricated Li/V_2O_5 based cell, Figures 18-21, although the VC reaction itself induced an impedance increase.

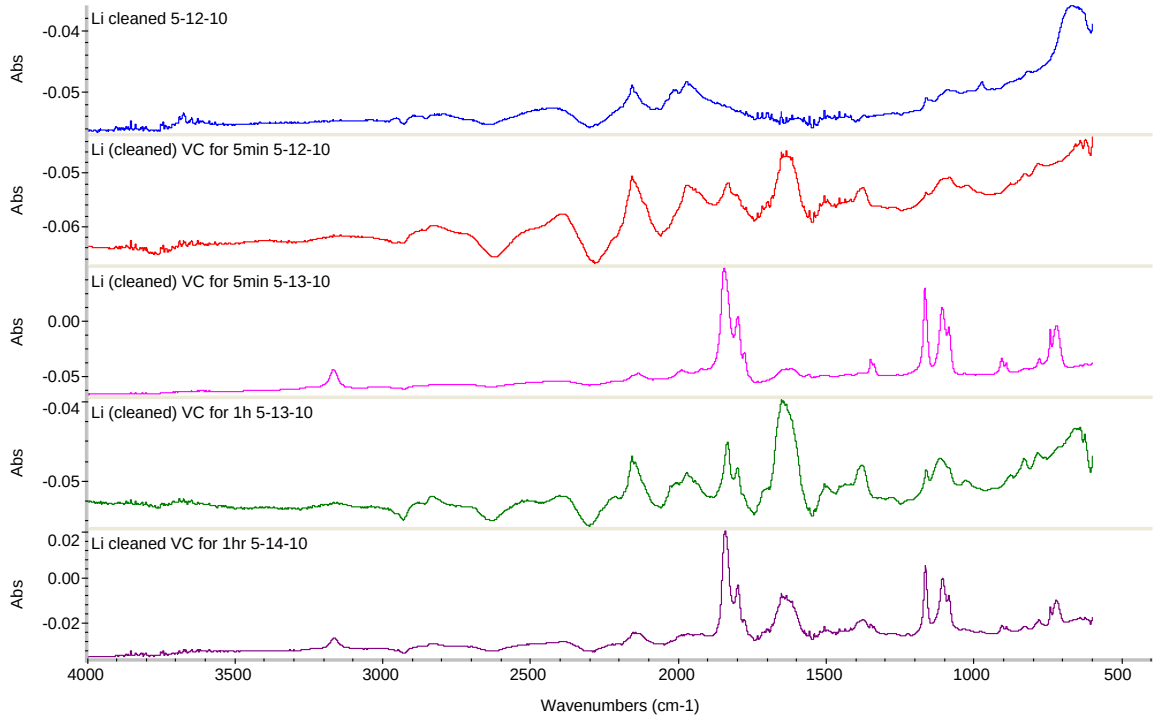

Figure 18. FTIR peaks approx 1800 and 1100 cm-1 indicates organic bonds related to VC polymerization on Li.

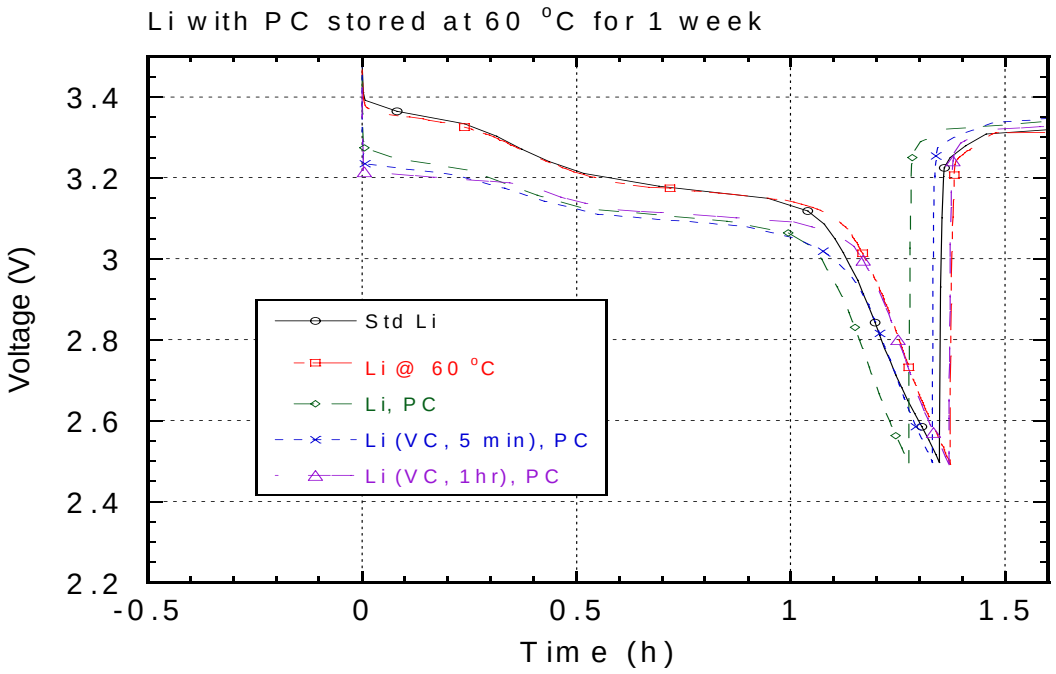

Figure 19. Li with PC stored at 60 °C for one week.

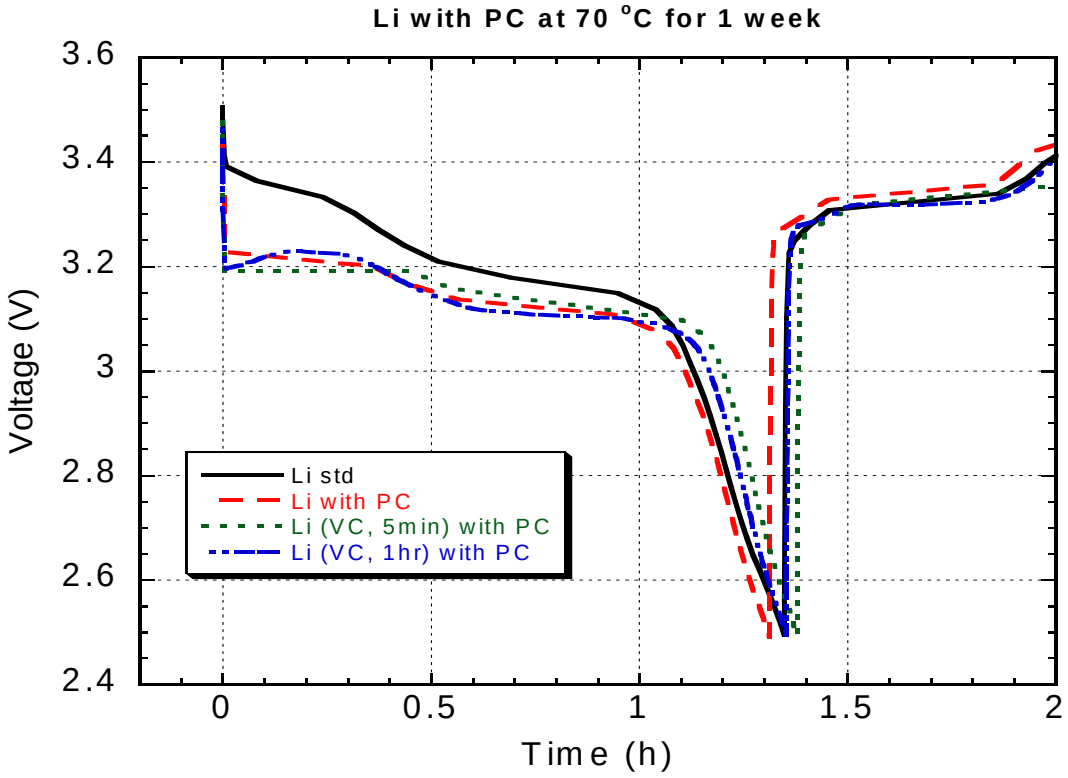

Figure 20. Li with PC stored at 70 °C for one week.

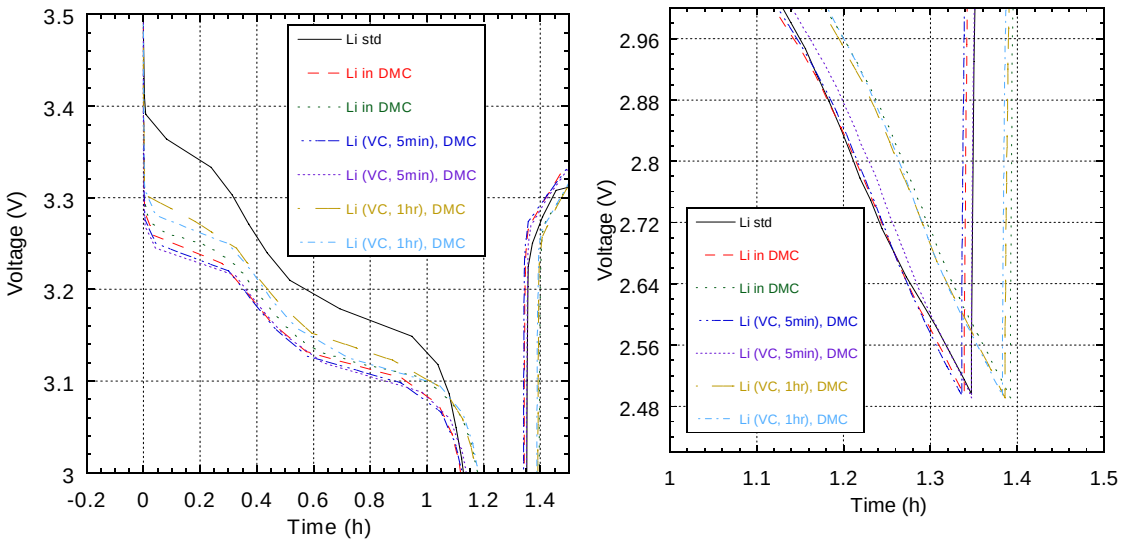

Figure 21. VC treated Li in DMC at 70 ^{o}C for 1 week

Given that the results of the VC tests indicated that using VC was only a marginal improvement over not using any special method for prepassivation, in the end, we decided not to perform any special treatment to the lithium electrodes during the finally assembly of the battery.

Conclusion: *During Phase II, we have successfully conducted a series of tests to determine if vapor pressure from the electrolyte would have a negative effect on the performance of the electrodes, given the long term requirements of the reserve cell and the porous nature of the honeycomb membrane separator. Test results indicate that passivation techniques do have some positive effects but that the improvements are minimal, and do not warrant additional processing overhead over using a non-passivation lithium approach.*

TASK 5A. Battery Assembly - Assembly of final multi-cell battery, bonding of top and bottom sub assemblies

We attempted to perform and optimize the sealing operation at a reduced temperature of 150 ^{o}C, and initially tested bonding samples outside of the glove box environment, without the inclusion of the electrode stack or electrolyte. Samples' testing indicated that we were able to form a thermocompression bond at 150 ^{o}C, with compression force set at

90-200 lbs for 8 hours, but when we attempted to reproduce these results on the final battery assemblies containing the electrode stack, we were not able to obtain acceptable bond strength. An obvious solution to this problem would be increase the temperature to ~ 400 ^{o}C as is typically done, however, we remind the reader that the upper bound temperature limit is based on the melting point of lithium, 181 ^{o}C, and it cannot be exceeded without a complete disintegration of the assembly.

We experienced problems with the thermocompression bond when we tried it on the actual samples, prefilled with the electrode stacks and performed bonding inside the glove box. An acceptable bond was not reproducible and was often failed after minimal manual handling. In trying to determine why we were unable to perform a thermocompression bond, we considered the possibility that we were not getting uniform bonding temperatures throughout the assembly. We measured the temperature variations from the bottom of the battery assembly containing the electrodes and the top of the assembly housing the reservoir area, and attempted to factor in the temperature differential at the gold bound interface layer, which is located approximately 1.5 mm from the base of the battery fixture. Testing determined that there was some thermal loss through the fixture, and we attributed this as the glass walls comprising the electrode containment grid do not have high thermal conductivity. We attempted to compensate for this temperature variation by leaving the fixture under compression for a longer period of time, to achieve improved temperature equilibrium throughout the fixture, in the hopes of getting temperature of the Au interface layer close to the desired 150 ^{o}C. As indicated above, repeated attempts at getting proper adhesion were unsuccessful, and we hypothesize that the electrode stack, which contains a compression spring, may be exerting enough vertical mechanical force inside the cell, that it was sufficient to break the thermocompression bond. We think that this problem is exacerbated due to the very low bond temperatures we are attempting to use to avoid melting the lithium.

One approach to solving the low temperature bonding problem would be to substitute the lithium electrode for an electrode made of lithium alloy, which has a higher melting point than pure lithium. With additional development, thermocompression bonding would be the preferred method of bonding, given the long shelf life requirements of a reserve cell, but due to the time constraints of the project, this will need to be investigated at a later date.

As an alternate approach to resolve the issue of bonding the two subassemblies, we decided to use Surlyn, a polymer material from Dupont, which is widely used in the battery industry. It has very desirable bonding properties, with a melting temperature in the 100 ^{o}C range, and is chemically inert to the electrolyte of choice and the electrode materials used in our design. We created templates and cut the samples of Surlyn material to match up to the openings of the 3x4 arrayed battery cavities and overlaid the Surlyn gasket on the electrode portion of the battery fixture. We then carefully lowered the top sub assembly over the bottom, while the fixture was being assembled in the bonding tool. Once assembled, we set the bonder's parameters 150 ^{o}C for 30 minutes and applied 24 lbs of force to the top of the fixture to make sure that the two subassemblies were in close contact during bonding. We continued to apply force to the sample during this cooling phase and let the samples cool in the bonder until they reached 50 ^{o}C. Inspection of the samples indicated a good bond at the interface.

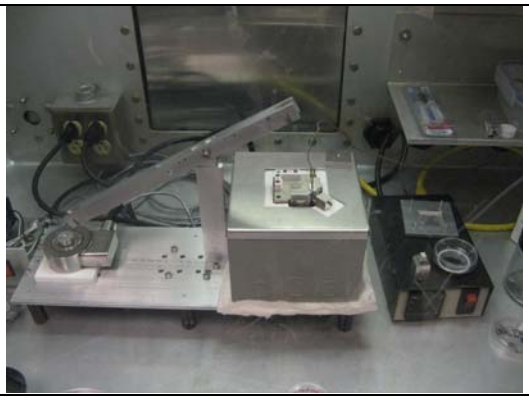

Figure 22. Glove box working environment and thermo compression bonder inside the glove chamber.

Conclusion: *We successfully assembled a fully functional multi-cell battery using a low melting temperature polymer as the bonding interface material between the top and bottom sub assemblies of the battery. With additional time available, optimization of this bonding interface can be improved by fine tuning the parameters, such that a thermo compression interface could be achieved.*

TASK 5B. Insertion of electrode stack

We created the electrode stack by inserting individual electrode elements into each cell of the 3x4 open array assembly while it was positioned on the bonder tool. The ordering of the layers was as follows, from the top down.

- CFx - ~ 680-705 microns
- Glass Separator - 250 microns
- Lithium foil – 300 microns
- Copper current collector – 25 microns
- Stainless steel compression spring - ~ 100 microns

The functionality of the stainless steel compression spring was to apply upward force on the electrode stack, and in particular, to keep the CFx electrodes, which are in contact with the gold metallization located on the bottom side of the porous honeycomb membrane. The gold contact on the membrane is designed to be the common positive current collector for each of the cells. In addition, the compression spring is intended to compensate for the reduction in size of the CFx material as it is consumed during discharge, so that it remains in contact with the common gold contact on the membrane.

Once all cells were populated, we used the Surlyn bonding process described in the previous section. Results of the bond on the assembled cells containing electrodes also showed good bonding characteristics.

Conclusion: *We have successfully built multiple 3x4 arrayed multi cell stacks containing active electrode materials, lithium and CFx, using a low temperature Surlyn bonding process.*

TASK 5C. Addition of electrolyte and sealing fill holes

After the Surlyn bonded samples had cooled completely, the reservoir cavities were filled with 100 micro-liters of electrolyte, consisting of 1M $LiClO_4$ with EC-DMC as the solvent. A syringe was used to dispense the electrolyte into each cell. Observations made during this phase of assembly revealed that it was rather challenging to dispense consistent amounts of electrolyte through the fill hole of each cell, due to the tendency of air bubble formation as air was displaced, while electrolyte filled the cell of the reservoir, and blocked the air from escaping from the fill hole. These observations were compounded due to the hydrophobic coatings inside the cell, which helped to repel the electrolyte from contacting the sidewalls of the cell, thus creating air pockets as it was being filled.

We attempted to modify the filling of the cells by placing a small amount of glass fiber wicking material into each cell, prior to filling, in an attempt to minimize the size of air bubbles from blocking the fill holes and to even out the level of the electrolyte as it fills the reservoir.

We speculate that further modifications to the top cap assembly could potentially reduce the air bubble formation issue, by the addition of a small vent hole located towards a corner of each cell, and positioned away from the fill hole, allowing air to escape while being filled.

Once filled with electrolyte, the tops of each fill hole were sealed off using Kapton tape, with the tape trimmed to just seal the fill hole, while still exposing the metallization layer surrounding each fill hole. Once all cells were sealed, silver epoxy was used to overcoat the Kapton tape, creating an airtight seal. This metallization is used as an external contact point outside each cell for triggering and electrowetting activation. Contact to the electrolyte is made through the conductive silicon material, which has a corresponding metalized contact region that is exposed to the electrolyte inside the cell.

Conclusion: *We have successfully created sealed reservoir chambers and filled each cell with the electrolyte of choice. We have observed that improvements can be made to the design of the top cap structure, by potentially modifying the structure with an additional vent hole at each cell, to help vent the air out of the cell as it is being filled with electrolyte. An air tight seal has been fortified using silver epoxy overcoat.*

TASK 5D. Attachment of printed circuit boards

Special printed circuit boards have been designed and fabricated to assist in battery characterization. Printed circuited boards were attached to the bottom and top of each 3x4 arrayed battery in order to aid in making wiring connections to each cells. The bottom circuit board provides negative and positive contacts for each cell during battery's use and discharge. The top circuit board provides contacts for applying the voltage triggering pulses, so that each cell can be addressed independently of each other.

Each battery array sample has two additional contact points, which are attached to the underside of the silicon porous membrane. These contact points act as common ground for triggering the cell and common positive current collector for the activated cell. Wiring connections are made to the membrane through an external contact point located on the underside membrane, which protrudes outside of the silicon and glass battery assembly. One wire is attached to the exposed gold area of the silicon membrane and the other contact point is attached to an exposed non metalized area of the underside of the silicon membrane.

The circuit boards are attached to the battery using silver epoxy.

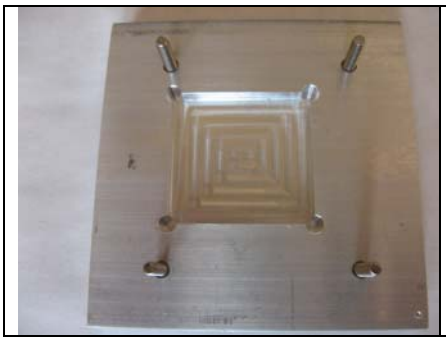

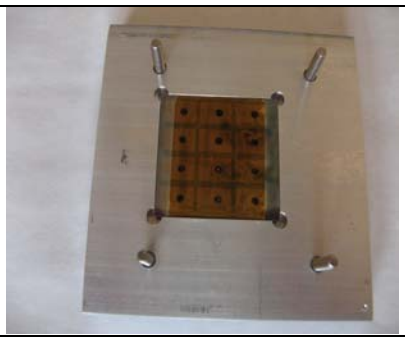

Figure 23. Alignment jig for mounting sample of the arrayed battery to printed circuit board.

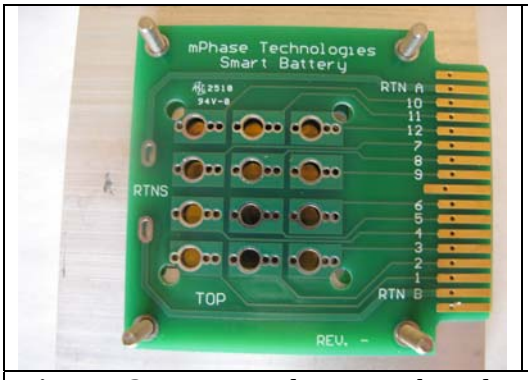

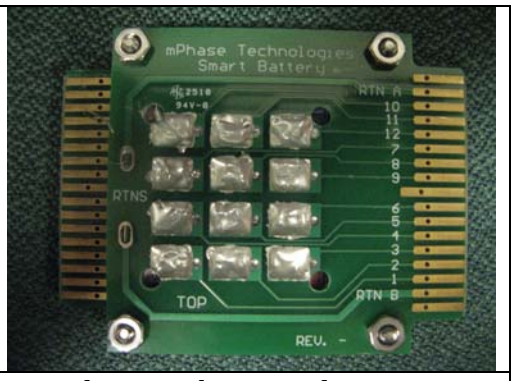

Figure 24. Printed circuit board mounted using battery alignment jig. Completed sample, 3x4 multi-cell batteries with attached top and bottom circuit boards. Battery is sandwiched between circuit boards.

Conclusion: *We successfully designed and attached printed circuit boards to assist in independently connecting each cell in the battery array. The circuit board allows us to trigger each cell via electrowetting and to receive output voltage from each cell after it has been triggered.*

Task 6. Discharging the cells of the multi-cell battery

After the battery was assembled and attached to printed circuit boards, it is now ready for triggering and discharging tests. The triggering has been accomplished by applying a 70 V, ~ 0.5 sec long voltage pulse to the desired cell. Activation has been observed by connecting the cell to the digital voltmeter to monitor voltage rise to 3-3.4 V. As in our previous reserve battery work, we observed fluctuating non-zero output voltages in the untriggered (reserve) state. However, the voltage drops down to zero as soon as a smallest load is applied to the cell, indicating that it is a spurious reading and is not an indication of a self-triggered cell.

We observed a somewhat longer than expected activation time of the cell. We are currently investigating the reasons for this effect and may only speculate that air pockets trapped in the cell during electrolyte filling may block the electrolyte from evenly spreading inside the cell.

Once the cell has been triggered, it was connected to the Maccor tool to discharge at a known rate and to record the data as a function of time.

Given the limited amount of time we had left in the project after we completed the assembly of several (~ 10 full batteries), we are in the early stage of the battery

performance characterization. Our preliminary results indicate (Figure 25) that a triggered cell is capable of delivering power to the load that exceeds the requirements of the original solicitation (100 nA as requested vs. 40 μA observed). This current draw is only an intermediate step in our testing and we are confident that even higher current draws can be supported by our batteries.

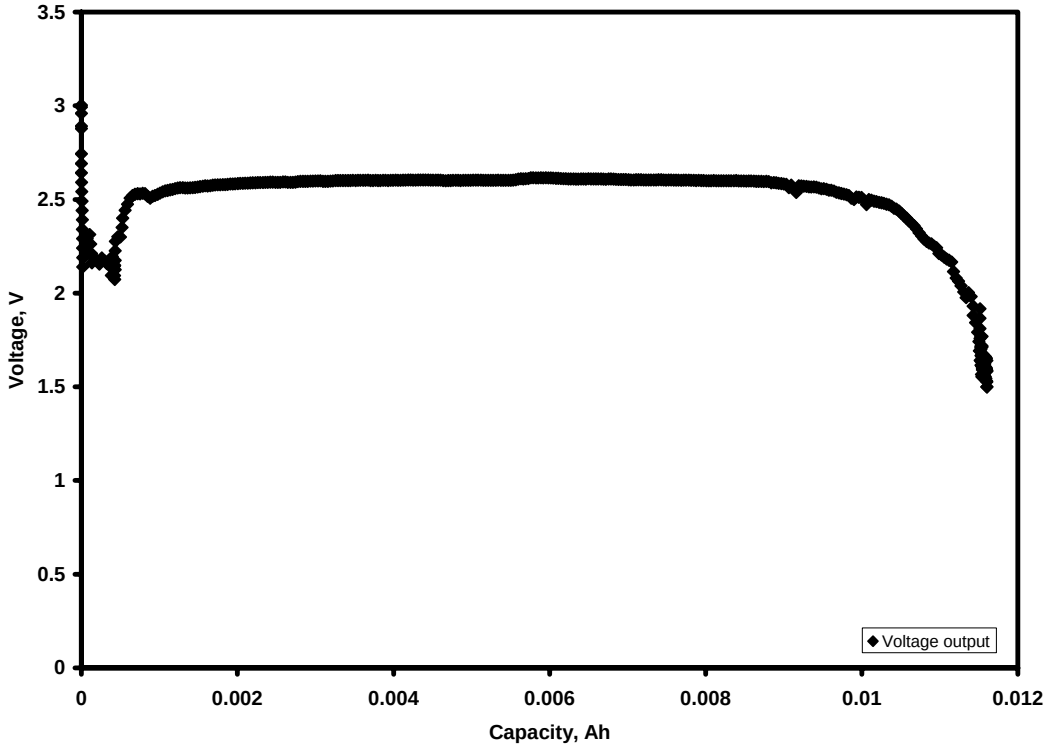

Figure 25. A discharge of a single cell in one of the fully assembled batteries. Capacity of ~ 10 mAh is demonstrated.

Data on Figure 25 suggests that a triggered cell behaves as expected, as is typical for a Li/CFx battery and that it has the capacity of ~ 10 mAh, which is in line and even exceeds the design capacity requirements of 3 mAh, which was proposed in the original solicitation using $Li/Mn0_{2,}$ in order to achieve 3 year active life per cell.

In the next round of testing we will continue testing individually triggered cells to characterize their performance across the temperature range and to ascertain their reproducibility.

Project Summary and Conclusion

During the course of the Phase 2 development program, we met our main objectives of developing a working prototype of 3x4 arrayed reserve micro-battery, in which each cell in the battery can be independently activated and individually addressed. The battery's design lends itself very well to supporting inherent power management for applications that require long shelf life and real world applications longevity, due to the reserve nature of each of the cells.

We have demonstrated that the battery can be designed to support commonly available lithium chemistries, (electrodes and electrolytes), providing for cells that output 3 V.

We have demonstrated that we can create syperhydrophobic and superlyophobic porous structures in silicon substrates using MEMS processing techniques, such that liquids having very low surface tension properties can be used in designs of reserve battery systems.

We created process flow and optimized process parameters for each layer in the battery assembly process on the wafer level, so that the all of the components of the battery can be outsourced to a commercial foundry partner.

We have demonstrated that activation of the cells can be accomplished by electrowetting, which allows for triggering and activation of the reserve battery without the need to physically breach a solid barrier as is required in a traditional reserve cell.

We have demonstrated integration of Li material and Li deposition technology into the mainstream MEMS and nanofabrication process flows.

We have demonstrated that the fully assembled cell can be successfully discharged under load.

We have demonstrated that the battery cells using the Li/CFx electrode stack exceed the design capacity requirements of 3 mAh per cell, which was proposed in the original solicitation in order to achieve 3 year active life per cell.

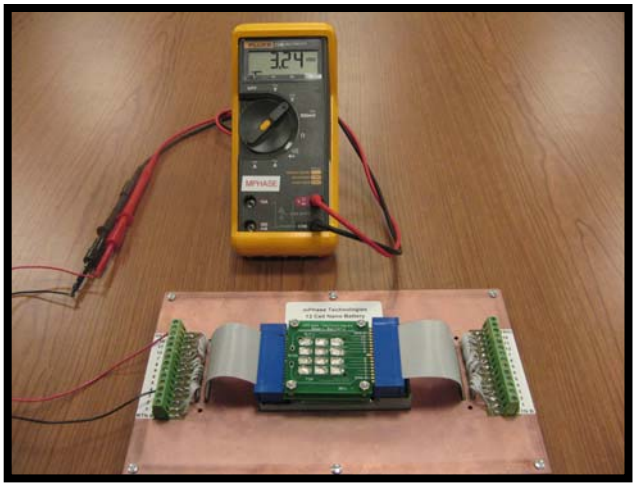

Figure 26. Test configuration showing results of a single cell after it has been triggered by electrowetting. Open cell voltage reaches to 3.24 volts, which is the expected voltage for this chemistry.